(2)

PENNSTATE

A Study of Gas Phase Chemistry of Solid Propellants Using a Microprobe Mass Spectrometer System

Third Annual Report:
Results for RDX, BLX-9, XM-39, M9 and JA-2

Thomas A. Litzinger

ONR Grant No. N00014-89-J-1238
Under supervision of Dr. R.S. Miller

College of Engineering
Department of Mechanical Engineering
University Park, Pennsylvania

(2)

A Study of Gas Phase Chemistry of Solid Propellants Using a Microprobe Mass Spectrometer System

Third Annual Report:
Results for RDX, BLX-9, XM-39, M9 and JA-2

Thomas A. Litzinger

ONR Grant No. N00014-89-J-1238
Under supervision of Dr. R.S. Miller

Table of Contents

SUMMARY

This research program is designed to address the critical need for data on the gas-phase chemistry of solid propellants through the development and application of a microprobe mass spectrometer (MPMS) system. The MPMS system is being used to study the gas-phase chemistry occurring above solid propellant ingredients and actual solid propellants when they are heated and/or ignited by the heat flux from a CO_2 laser. In addition to the MPMS system, direct and Schlieren photography are being used to study the flame structure and twenty-five micron thermocouples are being used to measure the gas-phase temperature profile During the last year nearly fifty tests were performed with neat RDX as well as with composite, XM-39 and BLX-9, and double-base propellants, M-9 and JA-2 .

Measurements of gas-phase species and temperature profiles for neat RDX and two RDX composite propellants show that while the chemical species detected are similar, the gas-phase structure for these propellants is significantly different. For incident laser energy fluxes above 100 W/cm^2, all three propellants exhibited a primary flame caused by the reaction of CH_2O and NO_2. The mole fraction of CH_2O at or near the sample surface was approximately 0.20 for RDX and XM39 but was about 0.33 for BLX9 due to the addition of CH_2O from the decomposition of the BTTN energetic plasticizer. The primary flame products consisted of significant amounts of NO for all three propellants and CO for the composites along with smaller amounts of H_2O for RDX and BLX9, CO_2 for RDX and XM39, and H_2 for RDX. At a heat flux of 200 W/cm^2, the location of the primary flame occurred at about 200-300 μm above the sample surface for neat RDX but was at 0.7-0.8 mm for BLX9 and 2.75-3.0 mm for XM39. A surface temperature of 550 K was observed for RDX and XM39 for laser heating without ignition. The "dark zone" temperature for BLX9 was approx. 1450 K but only 1120 K for XM39. Based on chemical species profiles, the RDX monopropellant exhibited a secondary flame zone immediately following the primary flame zone. BLX9 also had a secondary flame at heat fluxes above 200 W/cm^2 located 3.5-4.0 mm above the sample surface. XM39 did not display this secondary flame at any incident heat flux level tested.. The species profiles through the secondary flame showed HCN and NO being consumed while H_2, CO_2, N_2, and CO were produced.

In the investigation of the double-base propellants, the gas phase chemical structure of two nitrate ester propellants, M9 and JA-2, were studied. Because of the small thickness of the primary reaction zone and the current test configuration, only the basic dark zone chemical characteristics of M9 and JA-2 could be quantified. In these investigations, the temperature profiles of the propellants were found to be very similar, with the dark zone temperature of approximately 1800 K being reached within approximately 100μm of the burning surface. When the probe was positioned as close to the surface as possible at ignition, the results from the ignition transient showed gaseous species typical of the fizz zone. The detection of fizz zone species is probably due to the fact that the primary flame requires a short time to establish itself after the heat flux is applied to the surface of the propellant. For JA-2, the reduction of NO and production of CO in the dark zone appears to be more rapid than for M9. However, the amount of molecular hydrogen produced by M9 was twice that produced by JA-2. The amount of CH_2O and NO_2 detected in the dark zone of JA-2 were greater than that found in the dark zone of M9, suggesting that the primary flame of M9 burns more completely than the primary flame of JA-2. Finally, although an increase in laser heat flux increases the burning rate, it does not significantly change the gas phase chemistry occurring in the dark zone of nitrate ester based propellants.

INTRODUCTION

This research program is designed to address the critical need for data on the gas-phase chemistry of solid propellants through the development and application of a microprobe mass spectrometer (MPMS) system. The MPMS system is being used to study the gas-phase chemistry occurring above solid propellant ingredients and actual solid propellants when they are heated and/or ignited by the heat flux from a CO_2 laser. Currently the MPMS system uses quartz microprobes with orifice sizes of twenty microns which result in a spatial resolution of approximately 100 microns. In addition to the MPMS system, direct and Schlieren photography are being used to study the flame structure and twenty-five micron thermocouples are being used to measure the gas-phase temperature profile. Details of the experimental set-up can be found in the last two annual reports.

The specific goal of this research is to obtain detailed species profiles of the major reacting species above the surface of individual propellant ingredients and actual propellants in order to obtain an improved understanding of the controlling chemical processes and of the interactions of binders and oxidizers in heterogeneous propellants. In the testing both heterogeneous and homogeneous propellants are being studied as well as their individual ingredients. Over the last year testing continued with neat RDX, XM-39 and BLX-9, which are RDX based materials, and finally M-9 and JA-2, which are double-base propellants.

ENHANCEMENTS OF THE MPMS SYSTEM

During the last year several significant enhancements of the MPMS system capabilities were made. After considerable development work diatomic hydrogen was detected with the system. This capability is a significant because other measurement techniques including PLIF and FTIR cannot measure hydrogen, which is present in significant quantities and is potentially an important reactant. Secondly, calibrations for most of the major intermediate species have been performed so that the mole fraction of the various compounds can be determined. Calibrations for many species including H_2, CO, CO_2, NO and NO_2 were performed directly in the gas-phase, then calibration factors for other key species were calculated using these results and data on ionization cross-sections. Finally, new control and data reduction programs were

written for the mass spectrometer which have improved the flexibility of the MPMS and the reliability of the data reduction process.

EXPERIMENTAL RESULTS

Over the course of the last year nearly fifty tests were performed with neat RDX as well as with composite, XM-39 and BLX-9, and double-base propellants, M-9 and JA-2. In the following sections the results for neat RDX, BLX-9 and XM-39 will be summarized first and then the results for the double base propellants will be presented. These results were reported in two papers presented at the Twenty-eighth JANNAF Combustion Meeting[1,2].

RDX Monopropellant

Species profiles for deflagration of an RDX monopropellant under a heat flux of 200 W/cm^2 in argon at one atmosphere are displayed in Figure 1. These profiles are compilations from several different tests. At this heat flux, the primary flame zone occurs at about 200-300 μm above the sample surface and the secondary flame begins at a height of 500-600 μm. The slight separation of the two flame zones is believed to be due to the the laser-induced heating stretching out the spatial structure of the flame zones and preparation zones as mentioned by Parr and Hanson-Parr[3]. A violet-colored band about 200 μm thick was observed at the initiation of the secondary flame zone indicative of CN chemiluminescence[3,4]. N_2 and CO were not included in these graphs due to some difficulties in obtaining the species profiles from the signal intensity at 28 amu throughout the gas-phase structure, especially in the regions around the primary and secondary flame zones where species mole fractions and temperatures change quickly. However, tests conducted to resolve the mole fractions of N_2 and CO in the secondary flame zone showed the mole fraction of both CO and N_2 to be about 0.30. Also, analysis of the data for several tests at different ionization potential settings showed that very little N_2 exists in the gas-phase before it is produced in the secondary flame. The mole fraction of CO was found to be about 0.03-0.05 near the surface and was assumed to be roughly constant leading up to the secondary flame. These data for N_2 and CO were used to approximate profiles for them throughout the gas-phase

so that the mole fractions for the species depicted in Figure 1 could be calculated.

Figure 1 indicates that the primary flame zone reaction is principally due to the reaction of CH_2O and NO_2. The reaction produces a significant amount of NO and smaller amounts of H_2, CO_2, and H_2O. It is also believed that CO is produced to some extent in the primary flame. The reaction in the primary flame zone continues right up to the location of the initiation of the secondary flame as evidenced by the NO_2 profile. This structure corresponds well with results for a model by Melius[5] of the gas-phase flame chemistry of RDX that showed the luminous flame did not stand off from the primary flame but still maintained a spatial separation. Both HCN and N_2O remain relatively inert through the primary flame and are consumed in the secondary flame which starts at 500-600 μm above the surface. The primary reaction in the secondary flame is the reduction of NO by HCN which produces small amounts of CO_2, H_2, H_2O, and substantial amounts of CO and N_2 (not shown in Figure 1). Korobeinichev et al.[6] also observed this reaction for the deflagration of RDX at a pressure of 0.5 atmosphere of argon. Their initial mole fractions of NO and HCN were both 0.22 whereas Figure 1 displays the same mole fraction of NO at the start of the secondary flame but only a mole fraction of 0.15 for HCN. However, the trends in product species profiles are quite similar to those of Korobeinichev et al.[6]

Several interesting physical phenomena were observed for the ignition and combustion of neat RDX. As the RDX monopropellant is heated, the solid melts and forms a melt layer on the surface as reported by numerous researchers. In the high-speed videos, the surface appeared to grow slightly at the onset of laser heating as the melt layer was established. If the level of incident heat flux was above a critical value of 43±5 W/cm^2, the primary flame was established, leading to subsequent quasi-steady burning of the monopropellant. However, if the heat flux level was below this critical value, no flame was established and the melt layer "boiled" vigorously with large bubbles evolved from the condensed phase. The thickness of the melt layer also became quite large as the heating time was increased. As the incident heat flux was increased far above the critical value, the surface boiling became more steady and well defined with the melt layer appearing to become considerably thinner as the heat flux was increased. These changes with heat flux could indicate that at low heat fluxes there is sufficient residence time for the liquefied RDX to decompose and/or vaporize in the thick melt layer with secondary

reactions occuring between the evolved decomposition products, but as the heat flux is increased, the melt layer becomes thinner due to increased vaporization of the liquid and subsurface chemical activity decreases due to decreased residence time.

Temperature profiles were not obtained for neat RDX because the high flame temperatures immediately burned out the fine-wire thermocouples. However, measurements were obtained for the surface temperature in tests below the critical heat flux where the flame zones establish. The surface temperature was 550 K for these no-ignition tests. Melius[5] calculated a surface temperature of 549K in his model of RDX combustion at one atmosphere. For tests where the primary flame was established, a rapid rise in temperature was observed as the thermocouple left the melt layer, but the thermocouple was quickly burned out due to the intense flame. This rapid rise in temperature directly above the surface is believed to be indicative of the decomposition of gaseous RDX and/or large fragments from the RDX molecule. Modifications of the current setup are being made so that thermal profiles for the RDX monopropellant can be obtained up to the final flame zone.

XM39 Composite Propellant

The species profiles for deflagration of XM39 are given in Figure 2. Reaction of CH_2O and NO_2 characteristic of the primary flame zone slowly takes place as the gases move away from the surface and the rapid reactions characteristic of this zone occur far from the surface at around 2.5 mm and extends to 3 mm. No secondary flame was observed at any level of incident heat flux in argon at one atmosphere. CO was resolved with a high level of confidence at an ionization energy of 18 ev, but difficulties were still encountered in resolving N_2. However, the binders CAB ($C_{15}H_{22}O_8$) and ATEC ($C_{14}H_{22}O_8$) that comprise almost 20% of the propellant mixture contain no nitrogen, and the remaining 4% of nitrocellulose contained in the propellant is not expected to substantially contribute to the amount of N_2 in the gas-phase. Thus, the amount of N_2 before the secondary flame is expected to be minimal as it is for neat RDX.

Overall, the products of this primary flame are similar to those seen in RDX combustion with the CH_2O and NO_2 reacting to form NO, CO, and CO_2. The mole fraction of H_2O is observed to change very little through the gas-phase and is also only about half of the mole

fraction for H_2O found in Figure 1. This concentration is less than expected so additional experiments will be performed to verify the result. The mole fraction of H_2 was only around 0.005 throughout the distance profiled and thus was not included in Figure 2. The species profiles displayed in Figure 2 only go to within 750 μm of the surface due to residue buildup on the sample surface that disrupts the gas sampling.

The mole fraction of NO_2 at 0.75 mm above the surface is about 1.7 times the mole fraction observed at the surface of RDX. This may be partly due to additional NO_2 evolved from decomposing nitrocellulose. The mole fraction of CH_2O at 0.75 mm is almost exactly the same as that observed the surface of RDX. A considerable amount of CO is produced in the primary flame leading to a mole fraction of 0.33 at 4.5 mm. The amount of CO at 0.75 mm from the surface is also quite substantial with respect to the amount observed near the surface of RDX. NO peaks at nearly the same mole fraction for both XM39 and RDX. Based upon their chemical structures, the binders CAB and ATEC can contribute the additional CO but they have no nitrogen to offer to form NO. Apparent production of HCN was also observed in the primary flame region for deflagration of XM39 as seen in Figure 2. To the authors' knowledge, this production has never before been reported. Fundamental studies of the CH_2O/NO_2 reaction[2,5] have shown no evidence at all for the production of HCN from this reaction. Thus, another mechanism must be responsible for its production.

Several tests were conducted at low heat fluxes of 35-50 W/cm^2 with the microprobe directly on the sample surface to investigate the pre-ignition evolution of gases directly from the surface. Upon laser heating, NO_2, NO, and HCN were evolved from the surface in a preignition "puff". These species are simple molecules than can be derived directly from scission of the N-NO_2 bond and C-N bonds in the ring structure along with evolution of H and O atoms from bonds to C and N, respectively. The concerted dissociation scheme proposed by Zhao et al.[8] lists these molecules except for NO and also includes HONO. A small peak at 47 amu was observed, which may represent HONO, although this molecule is highly reactive and very difficult to detect. Small peaks were also observed at molecular weights of 52, representing C_2N_2, and at 73, which is believed to be an ionizer-induced fragment of N-nitroformimine (CH_2NNO_2) at 74 amu. As the sample was heated, the gases were evolved and detected and then the melt layer began to grow and eventually immersed the probe tip. It is interesting to note that the peak at 73 grew

as the melt layer began to immerse the probe, which suggests that there may be decomposition in the condensed phase of the RDX molecule producing the N-nitroformimine fragment of the ring structure as proposed by several researchers. However, this is only preliminary data that requires further investigation.

A temperature profile is displayed in Figure 3 for deflagration of XM39 with an incident heat flux of only 100 W/cm^2. This profile shows the rapid primary flame reaction peaking beginning at about 3.25 mm. It is expected that this rapid temperature rise coincides with abrupt changes in species profiles displayed in Figure 2. It might be inferred from this data and the location of the maximum rate of species production at about 3 mm in Figure 2 that lowering the heat flux increases the height of the primary flame. This could be due to the decrease in energy available to pyrolyze the propellant and heat the gaseous species to the temperature required for fast reaction, but more tests at different heat fluxes are needed to verify this effect. The temperature profile exhibits interesting trends at the surface. Upon laser heating the surface temperature rapidly rose to 550 K as was also measured for RDX. Upon ignition and subsequent regression of the surface, the temperature rapidly rose to 650 K and then up to 700 K at 100 μm above the surface. This rapid rise in temperature near the surface is indicative of the decomposition zone where RDX and binder molecules decompose. After the decomposition zone, the temperature slowly rises corresponding to the slow reacton of NO_2 and CH_2O until rapid reaction occurs at 920 K with the temperature jumping to 1090 K and peaking at 1130 K at 4.5 mm.

BLX9 Composite Propellant

Figure 4 displays the chemical species profiles for deflagration of BLX9 at 200 W/cm^2 in argon at one atmosphere. For this composite propellant, the CH_2O + NO_2 reaction characteristic of the primary flame zone slowly begins just above the sample surface and the rapid reaction zone is centered at about 0.7-0.8 mm above the surface. The products of the primary flame are CO and NO with a small amount of H_2O also produced. As was mentioned for the tests of XM39, the mole fraction of H_2O appears to be lower than expected. N_2 was once again excluded due to difficulties in quantifying its profile and also because it is not believed to be a major species in the primary flame region. The mole fraction of HCN was once again

observed to rise to some extent through the primary flame region. A secondary flame zone was also observed at 3.5-4.0 mm above the surface with the same fundamental chemistry as for the secondary flame of RDX. This zone has not been thoroughly quantified as of yet and therefore was not included here.

It is quite interesting to note that the mole fraction of CH_2O present at the sample surface is almost 1.5 times that observed for RDX and XM39 at or near the surface. This is due to the energetic plasticizer BTTN which is almost 25% of the total ingredients in the composite BLX9. BTTN has a structure containing two CH_2O groups, one HCO group, one CH_2 group, and three NO_2 groups. Thus, it is apparent that BTTN can substantially contribute to the CH_2O mole fraction. The NO_2 mole fraction at the surface of BLX9 was also about 1.3 times higher than that for neat RDX, which also is due to the BTTN. The increase of the mole fractions of CH_2O and NO_2 near the surface by the BTTN may be responsible for the primary flame being located much closer to the surface than for XM39.

Temperature profiles were also obtained for BLX9 up to the secondary flame zone. A surface temperature of about 720 K has previously been reported from work conducted in this lab[9]. The temperature quickly rises to 790±20 K just above the sample surface and then slowly rises to 1100 K where the rapid primary flame reaction causes the temperature to rise to a dark zone temperature of 1400 K. This temperature is about 300 K higher than the temperature observed after the primary flame for XM39 (see Fig. 3).

Double base Propellants

The first mass spectrometer tests performed on the propellants were molecular mass scans to determine the major and minor molecular masses that would be detected by the mass spectrometer. These tests were performed in argon at one atmosphere with an incident laser heat flux of 100 W/cm^2. All of the tests were performed with the probe starting at the surface of the propellant. With the initiation of the laser heating, the burning propellant was pulled away from the probe at 2 mm/sec. The test samples typically took approximately two seconds to completely burn, at which time the test would end. Table 1 contains a complete list of major and minor molecular masses detected by the mass spectrometer during these tests. A major molecular mass

peak was defined as producing a maximum signal during the test of greater than 500 mv, while the definition of a minor peak was any observable peak from a test under 500 mv.

Table 1: Molecular mass peaks detected in molecular mass scans

	M9	JA-2
Minor Molecular Mass Peaks	2, 14, 15, 16, 17, 26, 27, 31, 32, 36, 39, 41, 42, 43, 45, 46, 47, 52, 55, 56, 58, 68, 72, 78	2, 14, 15, 16, 17, 26, 27, 31, 32, 36, 39, 41, 42, 45, 46, 47, 53, 54, 55, 56, 57, 58, 60, 68, 71, 72, 73
Major Molecular Mass Peaks	18, 28, 29, 30, 44	18, 28, 29, 30,44
Quantified Molecular Mass Peaks	2, 18, 28, 29, 30, 31, 44, 46	2, 18, 28, 29, 30, 31, 44, 46

In comparing the data obtained from M9 and JA-2, several interesting observations were made. Since these tests were performed with the probe as close to the surface as possible at the initiation of the test, the data from the beginning of the test obviously is obtained during the ignition transient. Generally, M9 and JA-2 were observed to have very similar transient gas phase characteristics, with differences occurring once the probe was about a millimeter above the burning surface and steady state burning had been established. The first data points in these experiments were close to the fizz zone characteristics as indicated by relatively high concentrations of initial decomposition species such as NO_2 and CH_2O (approximately 20% and 10% of the detected composition, respectively) and the relatively low concentration of final product species such as H_2O, CO, NO, and CO_2 (approximateiy 10%, 15%, 25%, and 16% of detected composition, respectively). The initial decomposition products of the nitrate esters are apparently reaching the probe before the primary flame has had a chance to establish itself.

The next set of tests performed were intended to determine whether changing the incident heat flux to the surface of the propellant would cause any significant changes in the gas phase species profiles. The experimental conditions and parameters were identical to that of the 100 W/cm^2 tests, except that the incident heat flux from the CO_2 laser was increased to about 545 W/cm^2. It was found that the concentrations of gases observed in the high heat flux tests were nearly identical to those observed with the heat flux at 100 W/cm^2.

After the high heat flux tests, a final set of experiments were performed to determine the species profiles of the propellants when burning at steady state. The propellants were positioned

about one to two millimeters away from the probe. Once ignited, the samples were moved toward the probe until the probe contacted the surface of the propellant, which typically occurred about 400 milliseconds after the initiation of the test. Once the probe had contacted the surface of the propellant, the propellant would be pulled away at 2 mm/s until the end of the test. The incident heat flux in these tests was again set at 100 W/cm^2, and the orifice size of the probe was typically 30 μm, providing a sampling resolution of approximately 150 μm.

The species profiles obtained from the steady state burning tests are presented in Figure 5 for M9 and Figure 6 for JA-2. An interesting observation made was that the initial concentrations of fizz zone species were less for the steady-state burning cases than with the molecular mass scans. Since the molecular mass scans included the ignition transient, it is likely that the first few data points represent the initial decomposition products that made their way to the probe before the primary flame was established. However, in the steady state burning case the primary flame would have time to established itself.

Another interesting result from these tests involved the hydrogen trace. The results show that M9 produces about twice the hydrogen that JA-2 does. Also, the amounts of CH_2O and NO_2 detected in the dark zone of JA-2 were greater than that found in the dark zone of M9, suggesting that the primary flame of M9 burns more completely than the primary flame of JA-2. M9 is a 'hotter' (higher chemical heat of explosion) composition than JA-2 due to its greater nitroglycerin composition. Nitroglycerin, because of its greater NO_2 content by weight is more exothermic than any of the other nitrate esters. This difference in composition of M9 compared to JA-2 may be the reason for increased hydrogen production and more complete oxidation of NO_2 and H_2CO, but further investigations are required to establish the connection.

REFERENCES

1. B.L. Fetherolf, P.M. Liiva, T.A. Litzinger and K.K.Kuo, "Thermal and Chemical Structure of the Reaction and Preparation Zones for RDX and RDX Composite Propellants", 28th JANNAF Combustion Meeting, October 1991.

2. P.M. Liiva, B.L. Fetherolf and T.A. Litzinger, "Thermal and Chemical Structure of the Reaction and Preparation Zones for M9 and JA-2", 28th JANNAF Combustion Meeting, October 1991.

3. T. Parr and D. Hanson-Parr, "Species and Temperature Profiles in Ignition and Deflagration of HMX", Spring Meeting, Western States Section, The Combustion Institute, Provo, Utah, April, 1987.

4. M. C. Branch, M. E. Sadeqi, A. A. Alfarayedhi, and P. J. Van Tiggelen, "Measurements of the Structure of Laminar, Premixed Flames of $CH_4/NO_2/O_2$ and $CH_2O/NO_2/O_2$ Mixtures," Combustion and Flame, Vol. 83, pp. 228-239, 1991.

5. C. F. Melius, "The Gas-Phase Flame Chemistry of Nitramine Combustion," 25th Jannaf Combustion Meeting, CPIA Publ. 498,
Vol. II, October, 1988.

6. N. E. Ermolin, O. P. Korobeinichev, L. V. Kuibida, and V. M. Fomin, "Study of the Kinetics and Mechanism of Chemical Reactions in Hexogen Flames," Translated from Fizika Goreniya i Vzryva, Vol. 22, No. 5, pp. 54-64, Sept.-Oct. 1986, 0010-5082/86/2205-0544, Plenum Publishing Corp., 1987.

7. C-Y Lin, H-T Wang, M. C. Lin, C. F. Melius, "A Shock Tube Study of the $CH_2O + NO_2$ Reaction at High Temperatures," Int. Journal of Chemical Kinetics, Vol. 22, pp. 455-482, 1990.

8. X. Zhao, E. J. Hintsa, Y. T. Lee, "Infrared Multiphoton Dissociation of RDX in a Molecular Beam," Journal of Chemical Physics, Vol. 88, No. 2, January, 1988.

9. B. L. Fetherolf, J. U. Kim, T. A. Litzinger, K. K. Kuo, "CO_2 Laser-induced Pyrolysis and Ignition Processes of Nitramine Composite Propellants," Poster Paper, Presented at the 22nd Symposium (Int.) on Combustion, Seattle, WA, August, 1988.

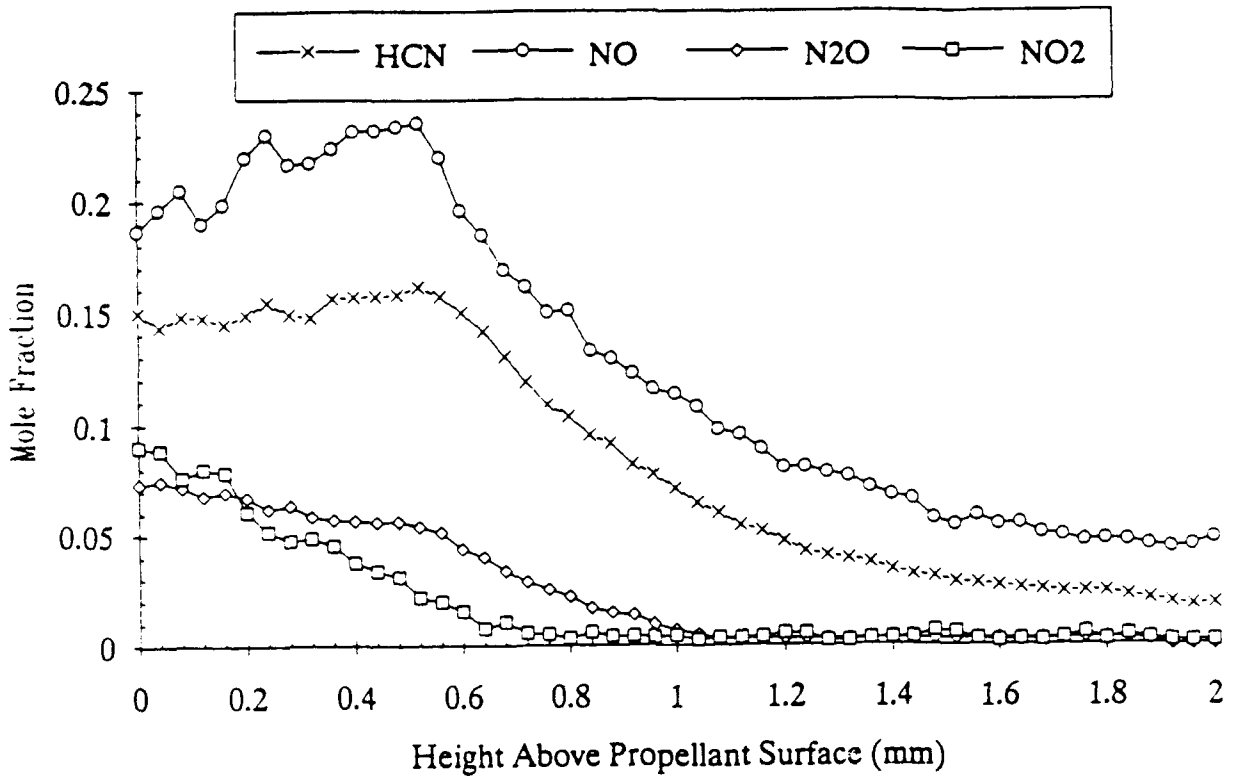

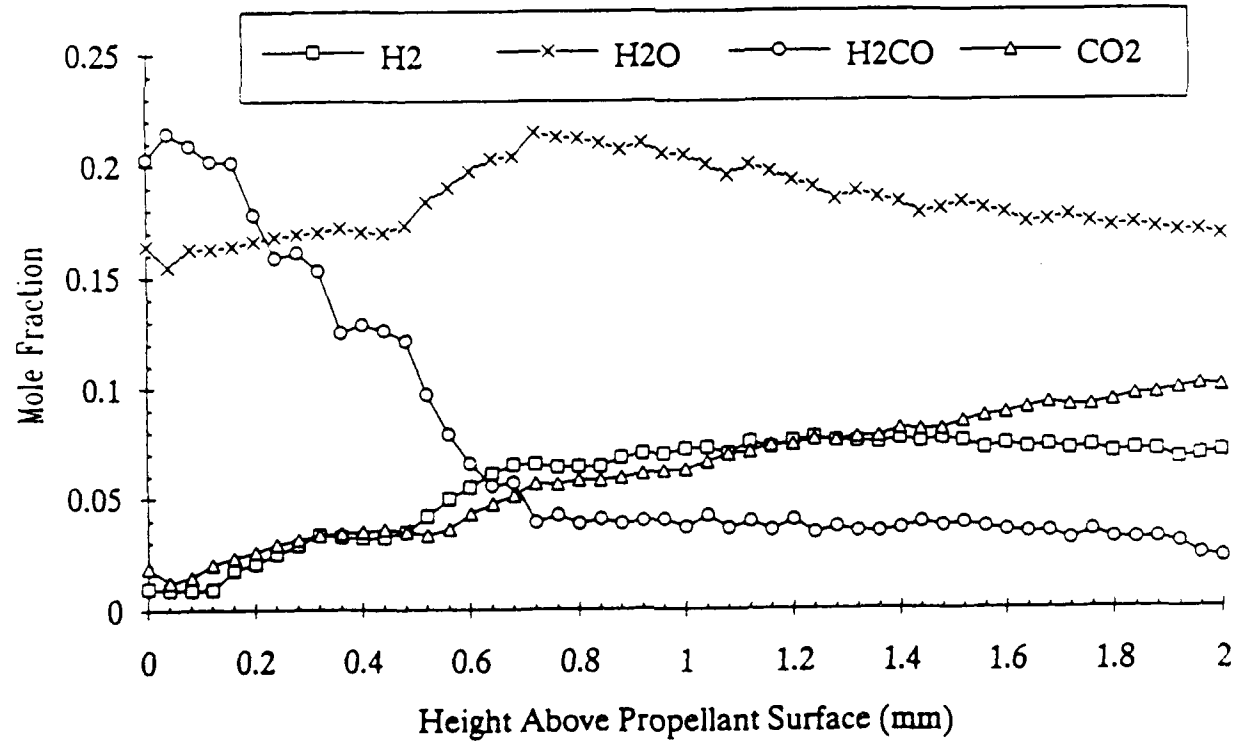

Figure 1. Species profiles for deflagration of RDX (q''=200 W/cm^2, P=1 atm of argon)

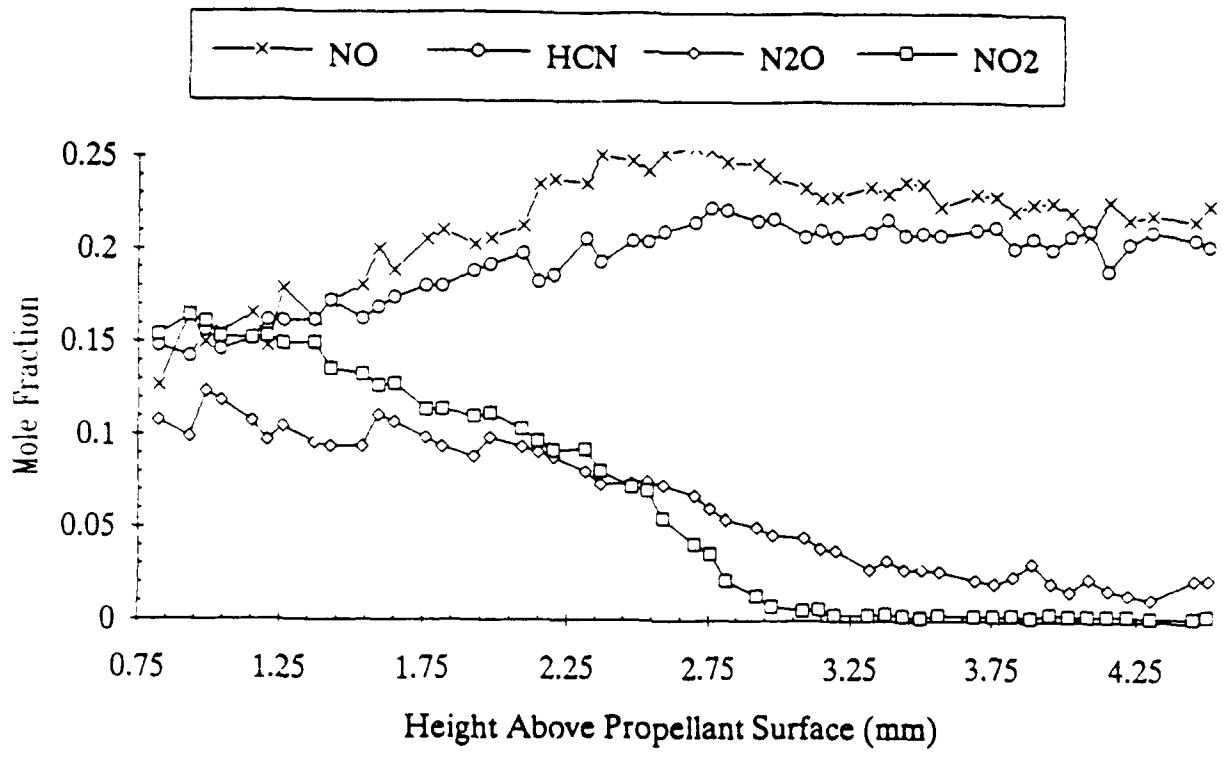

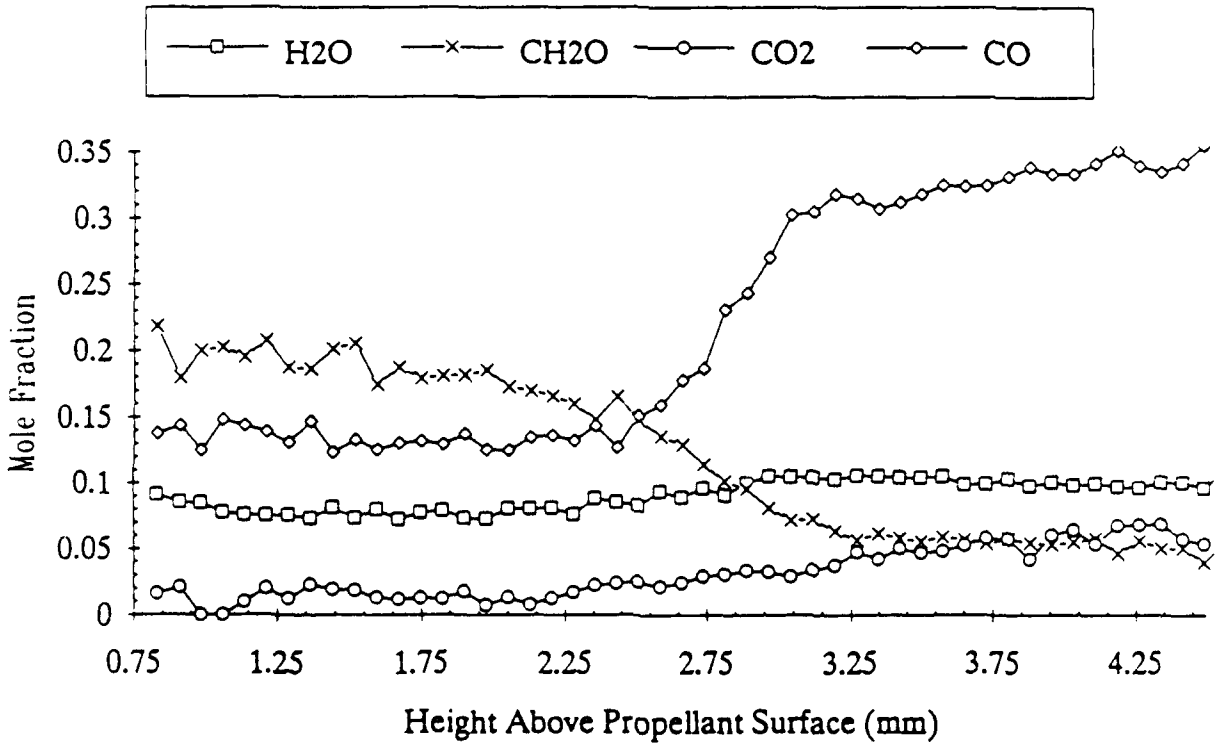

Figure 2. Species Profiles for Deflagration of XM39 (q''=200 W/cm^2, P=1 atm of argon)

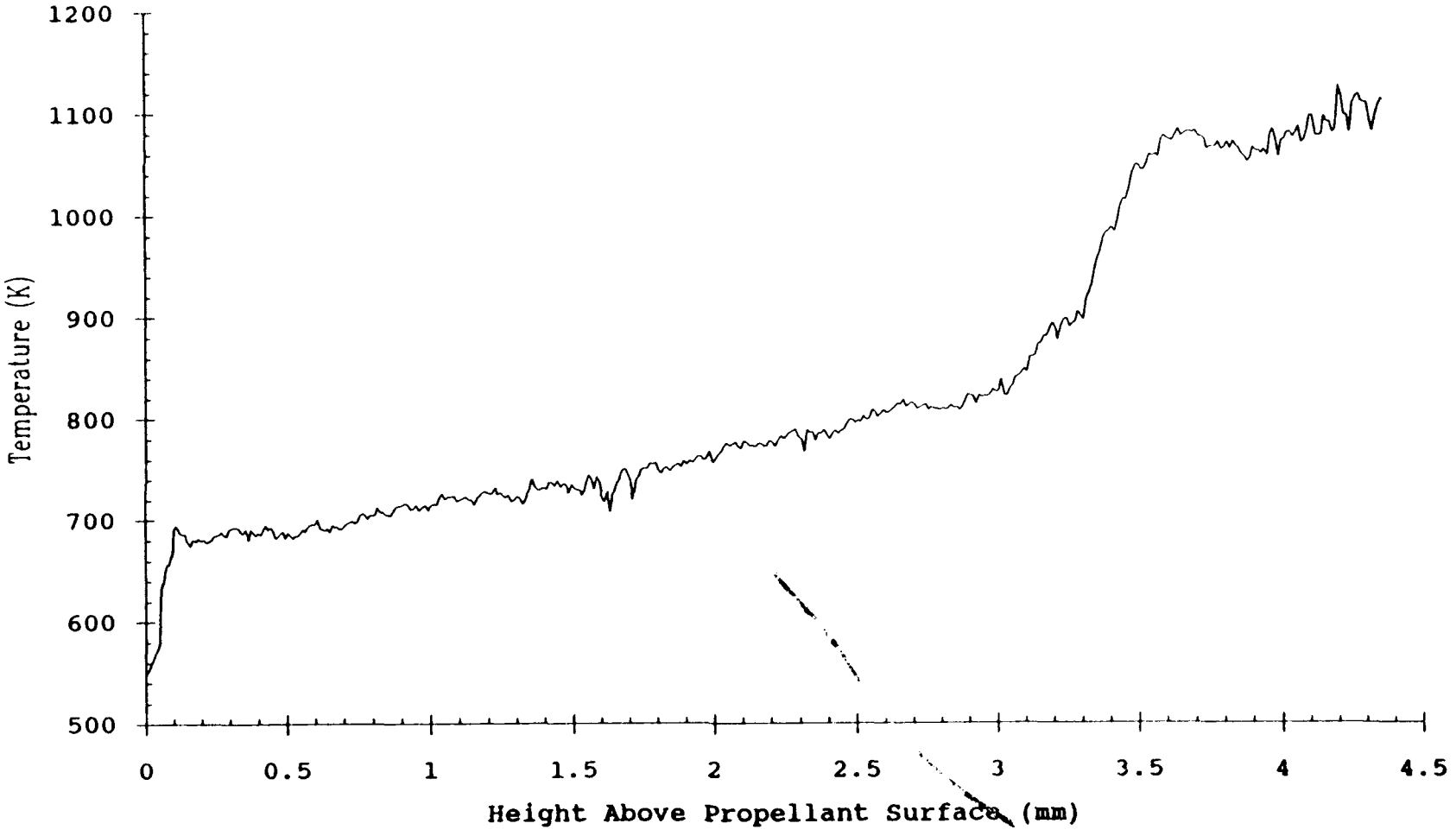

Figure 3. Temperature profile for deflagration of XM39 (q''=100 W/cm^2, P=1 atm of argon)

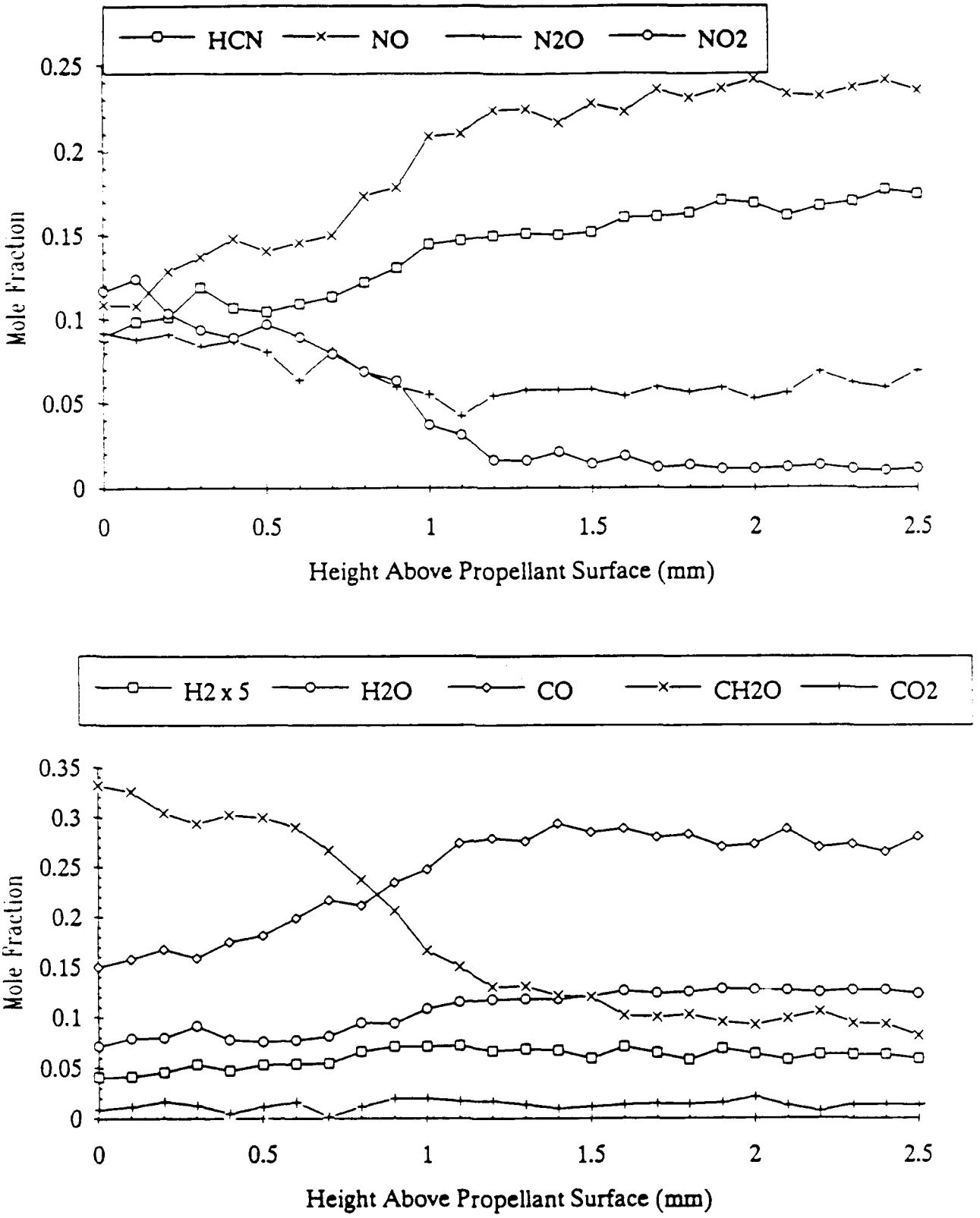

Figure 4. Species Profiles for Deflagration of BLX9 (q''=200 W/cm^2, P=1 atm of argon)

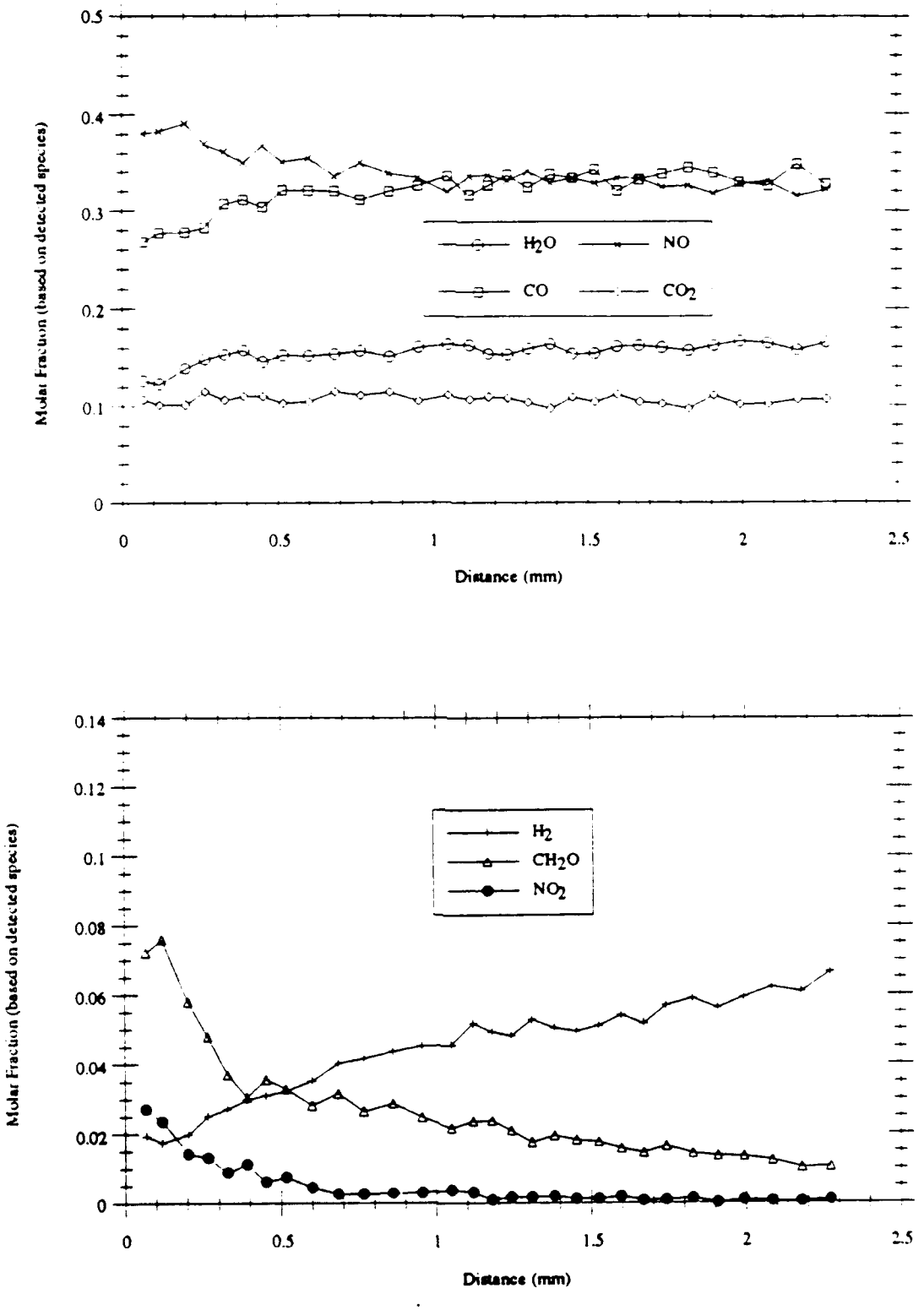

Figure 5. Species Profiles for Deflagration of M9 (q''=100 W/cm^2, P=1 atm of argon)

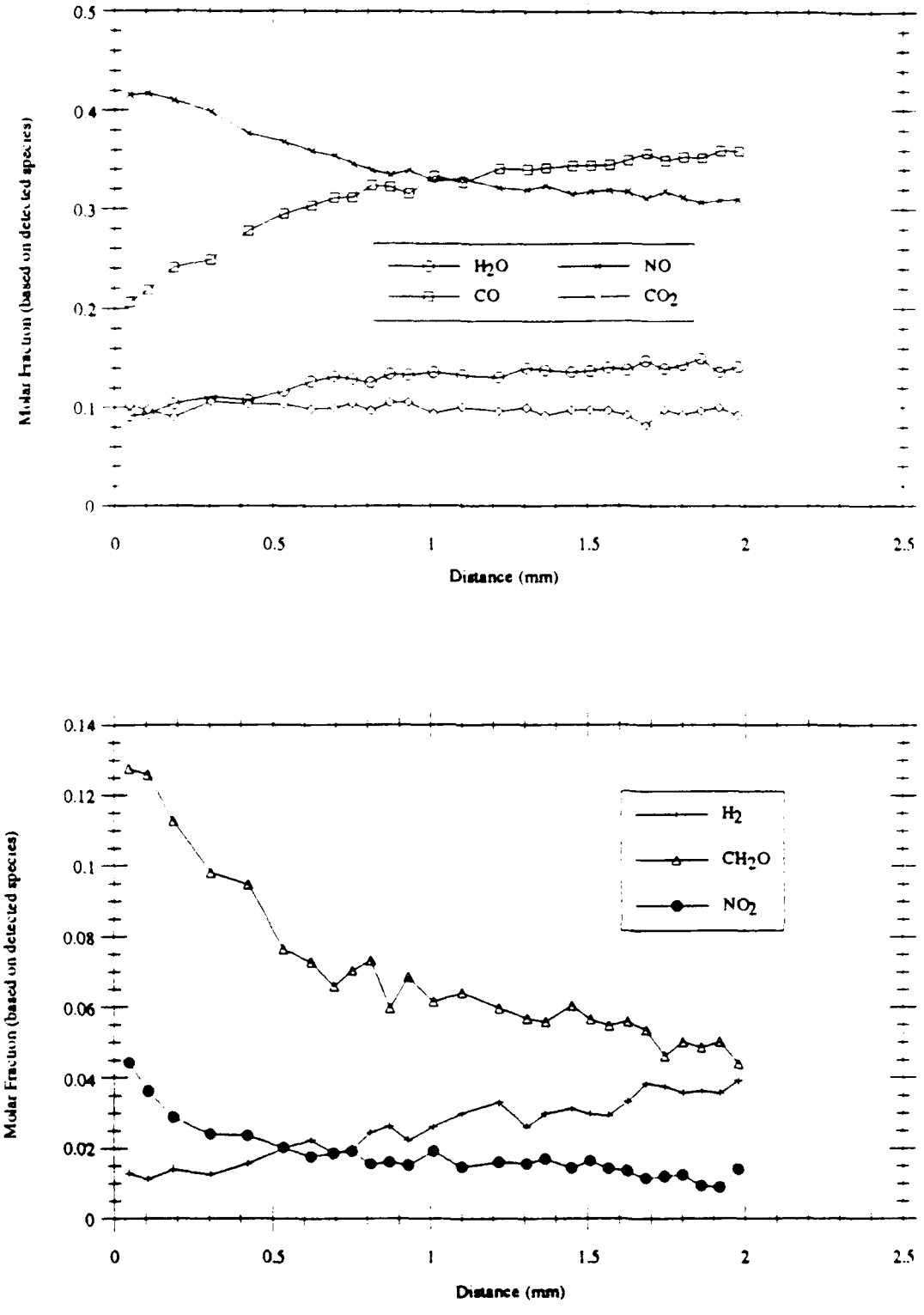

Figure 6. Species Profiles for Deflagration of JA-2 (q''=100 W/cm^2, P=1 atm of argon)